Journal of Mathematics and Statistics Studies
ISSN: 2709-4200
DOI: 10.32996/jmss
Journal Homepage: www.al-kindipublisher.com/index.php/jmss

JMSS
AL-KINDI CENTER FOR RESEARCH AND DEVELOPMENT

| RESEARCH ARTICLE

Comparing three recently developed techniques and using them to address the non-Newtonian fluid flow and heat transfer issue on a turbine disk

Ali Faris Abdulaali[1]✉ and Abdul-Sattar J. Ali Al-Saif[1]
[1]Department of Mathematics, College of Education for Pure Sciences, University of Basrah, 61001 Basrah, Iraq
Corresponding Author: Author's Name, Ali Faris Abdulaali, **E-mail**: ali.f.abdullah@uobasrah.edu.iq

| ABSTRACT

This study is investigating three distinct semi-analytical methods (SAGPM, q-HALPM, and PYRDTM) to solve nonlinear equations in the context of turbine cooling during heat transfer and fluid flow. These methods include Shehu, Laplace, and Young transformations and are improved by Padé approximation. The analysis not only explores how these methods deal with the complicated problems of cooling turbine systems but also remove to test efficiency, accuracy, and convergence of each of them. A comprehensive comparison of approximate solution methods to identify the most effective approach for modeling nonlinear thermal systems is conducted. The findings provide critical insights in to efficient analytical estimations for applications of the above recent methods. Ultimately, the results contribute to the advancement of accurate and computationally efficient solutions for complicated fluid dynamics problems, with broad applicability to various flow-thermal challenges. Moreover, the results showed that the methods are effective and powerful and give an indication that q-HALPM has superior convergence and high accuracy compared to PYRDTM and SAGPM.

| KEYWORDS

Fluid dynamics, SAGPM, q-HALPM, PYRDTM, Nonlinear thermal systems, Padé approximations, Computational efficiency, convergence, accuracy.

| ARTICLE INFORMATION

ACCEPTED: 18 July 2025 **PUBLISHED:** 02 August 2025 **DOI:** 10.32996/jmss.2025.6.3.6

1. Introduction

This study considers three advanced ways to solve complex equations to find the best method for getting accurate and reliable results while also being efficient with computing. The goal of the research is to make reliable estimates for complex thermodynamics and nonlinear mechanics problems by solving accuracy issues and improving solutions. The comparison study shows that the SAGPM, q-HALPM, and PYRDTM methods can create useful solutions, which helps us understand heat transfer and fluid flow better [1-2]. Their results matched numerical answers very well [3-5]. The Akbari–Ganji method [6] was further developed by Mirgolbabaee and others [8] in order to solve the nonlinear differential equations that control non-Newtonian fluid flow on a turbine disk in a symmetrical channel. This method was very close to the fourth-order Runge–Kutta method. At this time, Singh and Yadav [9] used the perturbation technique to examine the influence of different factors on the heat transfer and momentum equations of non-Newtonian fluid flow by employing the perturbation method. Their investigation brought out a strong correlation of temperature with Prandtl number and velocity with Reynolds number. In another study, Sheikhzadeh et al. [10] have solved the governing equations of the smooth non-Newtonian fluid flow in a porous-walled channel using the Galerkin and least squares methods. Comparing their results with the fourth-order Runge–Kutta method, they obtained good agreement and concluded that the Galerkin method was easier to implement and required less computation than the least squares method. Akinshilo et al. [11] studied the effect of heat on turbine disks and checked the validity of the analytical solutions by comparing them with numerical methods. They studied, by using two techniques—variational iteration and homotopy perturbation—the flow of a special fluid in a symmetric channel. To obtain an approximate solution for the non-Newtonian viscoelastic fluid flow through a circular channel, Al-Griffi and Al-Saif [12] applied the Yang transform combined with the homotopy perturbation method. Their study showed how the key factors influenced the main equations, and they found their results to be very close to

those obtained from numerical solutions. Lastly, Mohammed and Al-Saif [13] have introduced a novel approach to study the flow and heat transfer of non-Newtonian fluids on a turbine disk. The novel approach is called the Chebyshev homotopy perturbation method (CHPM), which is a combination of homotopy perturbation method and Chebyshev series. The result of this approach was compared with earlier studies that used numerical techniques. Semi-analytical approaches, therefore, in finding approximate solutions of complicated problems with strong nonlinearity, have become popular [14–19]. Semi-analytical methods are more precise and effective than traditional analytical methods, since these frequently become difficult due to complex nonlinear elements, while numerical methods may also be plagued with stability and convergence problems. Because they are very flexible, researchers find these methods especially interesting. They give a helpful way to study complex fluid movements, heat flow, and how materials act in engineering situations. Because of this, these methods are now important for solving tough real-world problems. These techniques, therefore, enable the researcher to develop control systems in such fields as fluid mechanics and heat transfer. In order to improve understanding and performance in such complex scenarios, there need to be accurate results [20]. This paper considered the thorny problem of cooling a turbine disk by using three methods: reduced differential transform method-Yang transform with Padé approximant (PYRDTM), q-homotopy-laplace transformation with Padé approximant (q-HALPM) and Shehu transformation-Akbari-Ganji's method with Padé approximant (SAGPM). This study aims at comparing all the results and pointing out which method is the best. These methods are very important; they may increase the accuracy of the analysis for the nonlinear problems [21]. That is particularly significant in certain disciplines, like fluid mechanics and heat transfer, whose solution requires high precision. Comparing among these various approaches will therefore let one determine precisely how each fares in sophisticated equations. This also provides guidance on how to steer future research concerning the selection of proper mathematical tools in engineering and science. The three techniques make the calculations easier by using integral transformations. In order to make the results look good, SAGPM uses the Shehu transform, the inverse transform, and the Akbari method for finding the approximate solutions. Before applying the Laplace transform and the Padé approximation, "q-HALPM" initiates with the q-homotopy approach. For the last approximation, it ends with the inverse Laplace transform. Finally, in order to make the final solutions more accurate, PYRDTM uses the reduced differential transform, Young's transform on both sides, and the Padé approximation. Comparing the results from the three methods, it was found that the q-Homotopy method has the best performance in view of the speed of convergence and the correctness of the results. This method had fewer major errors than the others, proving it is better. The q-homotopy method showed better accuracy and effectiveness compared to the other methods, although those methods gave good results. This study compares three advanced methods to find out the best way to gain accurate and reliable results and to be efficient with computing power. The objective of the research is to obtain reliable estimates for complex problems in thermodynamics and nonlinear mechanics by dealing with accuracy issues and enhancing solutions. It is clear from the comparative study that the SAGPM, q-HALPM, and PYRDTM approaches can achieve realistic solutions, and therefore, it deepens our understanding of the fluid flow dynamics and heat transfer mechanisms.

2. Mathematical formulation

2.1. Flow analysis

This study looks at how flow and heat transfer happen at the same time in a non-Newtonian viscoelastic fluid moving over a turbine disc for cooling uses. The problem is illustrated schematically in Fig.1, where the x-axis runs parallel to the disc's surface, and the y-axis is perpendicular to it. A porous disc at $y = L$ serves as one boundary, while the wall aligned with the r-axis is externally heated. The non-Newtonian fluid is uniformly injected through the perforated wall opposite the heated wall to provide cooling.

As shown in Fig.1, this cooling scenario for the turbine disc can be interpreted as a stagnation point flow with fluid injection. For steady, axisymmetric flow of a non-Newtonian fluid, the governing equations are as follows:

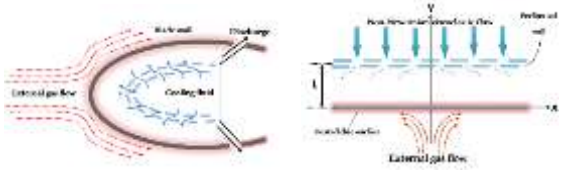

Fig. 1: A diagrammatic representation (right) illustrating the physical schematic of the problem (left).

The equations can be expressed in cylindrical coordinates as follows [7]

The continuity equation

$$\frac{\partial(x\,\mathcal{V}_x)}{\partial x}+\frac{\partial\left(x\,\mathcal{V}_y\right)}{\partial y}=0\ , \tag{1}$$

and the momentum equations

$$\mathcal{V}_x\frac{\partial\mathcal{V}_x}{\partial x}+\mathcal{V}_y\frac{\partial\mathcal{V}_x}{\partial y}=-\frac{1}{\beta}\frac{\partial\mathcal{P}}{\partial x}+\frac{1}{\beta}\left[\frac{\partial\eta_{xx}}{\partial x}+\frac{1}{x}(\eta_{xx}-\eta_{\theta\theta})+\frac{\partial\eta_{xy}}{\partial y}\right], \tag{2}$$

$$\mathcal{V}_x \frac{\partial \mathcal{V}_y}{\partial x} + \mathcal{V}_y \frac{\partial \mathcal{V}_y}{\partial y} = -\frac{1}{\beta}\frac{\partial \mathcal{P}}{\partial y} + \frac{1}{\beta}\left[\frac{\partial \eta_{yx}}{\partial x} + \frac{1}{x}\eta_{xy} + \frac{\partial \eta_{yy}}{\partial y}\right]. \quad (3)$$

The boundary conditions are given by:

$\mathcal{V}_x(x,0) = \mathcal{V}_y(x,0) = 0,\ \mathcal{V}_x(x,L) = 0,\ \mathcal{V}_y(x,L) = -U$ (4)

where $\mathcal{V}_x$ is the velocity in the x-direction, $\mathcal{V}_y$ is the velocity in the y-direction, β is the fluid density, P is the pressure, and η_{xx}, η_{xy}, η_{yx} and η_{yy} represent the components of the stress tensor. Here, U denotes the injection velocity of the fluid.

To address the axisymmetric flow case depicted in Fig.1, it is useful to introduce a stream function that inherently satisfies the continuity equation as follows:

$$\mathcal{V} = Ux^2\, f(\zeta)\,, \quad (5)$$

where $\zeta = \frac{y}{L}$ the velocity components in the *x*- and y-directions are then given by:

$\mathcal{V}_x = \frac{Ux}{L} f'(\zeta), \mathcal{V}_y = -2Uf(\zeta)\,.$ (6)

Using Equations (5) and (6), the momentum equations are derived as shown in [7]:

$$f'''' + 2Reff''' - k\,Re(4f''f''' + 2f'f'''') = 0 \quad (7)$$

with the boundary conditions:

$f(0) = f'(0) = f'(1) = 0,\ f(1) = 1\,,$ (8)

and Re is the Reynolds number, k is the injection Reynolds number.

2.2 Heat transfer analysis

In this problem, the dimensionless energy equation, which accounts for viscous dissipation, is expressed as follows [7]:

$$\Upsilon\mathcal{C}\left(\mathcal{V}_x\frac{\partial \mathcal{T}}{\partial x} + \mathcal{V}_x\frac{\partial \mathcal{T}}{\partial x}\right) = \mathcal{K}\nabla^2\mathcal{T} + \vartheta\,, \quad (9)$$

$$\vartheta = \eta_{xx}\frac{\partial \mathcal{V}_x}{\partial x} + \eta_{\theta\theta}\frac{\mathcal{V}_x}{x} + \eta_{yy}\frac{\partial \mathcal{V}_y}{\partial y} + \eta_{xy}\left(\frac{\partial \mathcal{V}_x}{\partial y} + \frac{\partial \mathcal{V}_y}{\partial x}\right), \quad (10)$$

here $\mathcal{C}, \mathcal{T}, \mathcal{K}$, and ϑ denote the specific heat, temperature, fluid coefficient, and dissipation function, respectively. When the effect of viscous dissipation is neglected, the equation simplifies to the following non-dimensional form:

$$g'' - Pr\,Re(n\,f'\,g + fg') = 0\,, n = 0,1,2,3,\ldots \quad (11)$$

subject to the following boundary conditions

$$g(0) = 1, g(1) = 0\ . \quad (12)$$

Here, Pr represents the Prandtl number, and n denotes the power-law index.

3. Approximate Methods Analysis

3.1. **Shehu transformation-Akbari-Ganji method with Padé approximation (SAGPM)**

Is served present a new simulation approach that combines effective, recent approximate analytical techniques: the Shehu transformation and the Akbari-Ganji method with Padé approximation (referred to as SAGPM). To summarize the algorithm of this method :

Consider the following nonlinear partial differential equation expressed in operator form:

$$\mathcal{L}(\mathcal{U}(x,y,t)) + \mathcal{R}(\mathcal{U}(x,y,t)) + \mathcal{N}(\mathcal{U}(x,y,t)) = z(x,y,t)\ , \quad (13)$$

with the initial conditions

$$\mathcal{U}(x,y,0) = c(x,y)\,. \quad (14)$$

where, $\mathcal{L}$ and $\mathcal{R}$ are linear differential operators involving partial derivatives, $\mathcal{N}$ is a nonlinear operator, and $z(x,y,t)$ represents an inhomogeneous term.

Step 1: Apply the Shehu transformation to both sides of Equation (13) to obtain:

$$S[\mathcal{L}(\mathcal{U}(x,y,t))] + S[\mathcal{R}(\mathcal{U}(x,y,t))] + S[\mathcal{N}(\mathcal{U}(x,y,t))] = S[z(x,y,t)] \quad (15)$$

By applying the differentiation property of the Shehu transformation along with the initial conditions, we obtain

$S[\mathcal{L}(\mathcal{U}(x,y,t))] = \frac{u}{v}c(x,y) + \frac{u}{v}S[z(x,y,t)] - \frac{u}{v}S[\mathcal{R}(\mathcal{U}(x,y,t)) + \mathcal{N}(\mathcal{U}(x,y,t))]$ (16)

Step 2: To proceed, we apply the inverse Shehu transformation to both sides of Equation (16), resulting in

$$\mathcal{U}(x,y,t) = Z(x,y,t) - S^{-1}\left[\frac{u}{v}S[\mathcal{R}(\mathcal{U}(x,y,t)) + \mathcal{N}(\mathcal{U}(x,y,t))]\right], \quad (17)$$

where $Z(x,y,t)$ represents the term arising from the source term and the prescribed initial conditions.

Step 3: Next, we represent and as Akbari-Ganji polynomials with constant coefficients, defined as follows

$$\mathcal{U}(t) = \sum_{k=0}^{n} a_k\ t^k \quad (18)$$

Substituting these polynomials into Equation (17) converts them to:

$(\sum_{k=0}^{n} a_k\ t^k) = Z(x,y,t) - S^{-1}\left[\frac{u}{v}S[\mathcal{R}(\sum_{k=0}^{n} a_k\ t^k) + \mathcal{N}(\sum_{k=0}^{n} a_k\ t^k)]\right]$ (19)

Using initial conditions, we determine some coefficients, and by further derivation of equation (23) and substitution of initial values, the remaining coefficients $a_i \; and \; b_i$ are obtained.

Step 4: Finally, we apply the Padé approximation of order $[i \,/\, j]$ to the power series solution generated by the SAGPM method. The values i and j are chosen as needed to obtain the final solution.

3.2. q-homotopy analysis method, Laplace transform and Padé approximant (q-HALPM)

The algorithm for the new methodology applied to differential equations builds upon the algorithms of the q-Homotopy analysis method (q-HAM), Laplace transform method (LTM), and Padé approximation method (PAM) as follows:

Step 1: Using the q-homotopy analysis method, the equation (13) becomes:

$$(1-nq)\mathcal{L}\big(\mathcal{U}(x,y,q)-\mathcal{U}_0(x,y)\big)-hq\mathcal{N}\big(\mathcal{U}(x,y)\big)=0 \;, \tag{20}$$

where $\mathcal{U}=\sum_{k=0}^{\infty}q^k\mathcal{U}_k$

By substituting $\mathcal{U}$ into Equation (20), we obtain a system of Equations in terms of the power series in q . Solving this system using integration yields the values of $\mathcal{U}$

The solution given by:

$\phi=\lim_{q\to\frac{1}{n}}\mathcal{U}=\sum_{k=0}^{\infty}\mathcal{U}_k\,(\frac{1}{n})^k \qquad ,n\geq 1$

Step 2: Take LT of ϕ , this leads to:

$$L[\phi(t)]=L\left[\sum_{k=0}^{\infty}\mathcal{U}_k\left(\frac{1}{n}\right)^k,t,s\right] \tag{21}$$

Step 3: We apply the Padé approximation to Equation (21) to obtain:

$$P_j^i(L[\phi(s)])=\text{Padé}\left\{L\left[\phi\left(\frac{1}{s}\right),[i,j]\right],1\leq i,j\leq i+j+1\right\} \tag{22}$$

Step 4: Finally, the inverse Laplace transform of Equation (22) is given by,

$\phi=L^{-1}\left[P_j^i\left(L\left[\phi\left(\frac{1}{s}\right),s,t\right]\right)\right]$

ϕ is an approximate solution.

3.3. Padé approximant-Yang transform with reduced differential transform method (PYRDTM)

To consider the nonlinear partial differential Equation in (13) applying present an algorithm for reduced differential transform method, referred to as PYRDTM, as described in the steps below:

Step 1: We apply the Yang transform to both sides of Equation (13) to obtain:

$$Y[\mathcal{L}(\mathcal{U}(x,y,t))]+Y[\mathcal{R}(\mathcal{U}(x,y,t))]+Y[\mathcal{N}(\mathcal{U}(x,y,t))]=Y[z(x,y,t)] \;. \tag{23}$$

Step 2: Applying the inverse Yang transform to both sides of Equation (23) yields:

$$\mathcal{U}(x,y,t)=Z(x,y,t)-Y^{-1}\big[sY[\mathcal{R}(\mathcal{U}(x,y,t))+\mathcal{N}(\mathcal{U}(x,y,t))]\big] \;. \tag{24}$$

where, $Z(x,y,t)$ represents the term generated by the source term and the specified initial conditions.

Step 3: Next, we apply the reduced differential transform method:

$$\tilde{\mathrm{U}}_0(x,y)=Z(x,y,t) \;, \tag{25}$$

$$\tilde{\mathrm{U}}_{n+1}(x,y)=-Y^{-1}\big[sY[\mathcal{R}(\tilde{\mathrm{U}}_n(x,y,t))+\mathcal{N}(\tilde{\mathrm{U}}_n(x,y,t))]\big] \;, \tag{26}$$

Here, $\mathcal{R}\big(\tilde{\mathrm{U}}_n(x,y)\big)$ and $\mathcal{N}\big(\tilde{\mathrm{U}}_n(x,y)\big)$ represent the transformations of the functions $\mathcal{R}\big(\mathcal{U}(x,y,t)\big)$ and $\mathcal{N}\big(\mathcal{U}(x,y,t)\big)$, respectively.

This approach combines the Yang transform with the reduced differential transform method. Using the YRDTM, we obtain the solution to Equation (13), with the initial condition (14), in the form of an infinite series that converges to the exact solution as follows:

$$\mathcal{U}(x,y,t)=\sum_{j=0}^{\infty}\tilde{\mathrm{U}}_n(x,y) \;. \tag{27}$$

Step 4: Finally, we apply the Padé approximant of order $[i/j]$ to the power series solution. The values of i and j are chosen arbitrarily. At this stage, the Padé approximant enhances the accuracy and convergence of the truncated series solution by expanding the domain of the solution.

4. Applying the approximation methods

In this section, we will apply the three approximate methods to the mathematical model (7,11), in order to clarify the basic steps for applying each method as follows:

4.1. SAGPM:

Now we will take the model in the Equations (7,11) to apply the method to it as follows:

By taking Shehu transformation on both sides of (7,11), we get

$$F(v,u)=\frac{u}{v}f(0)+\frac{u^2}{v^2}f'(0)+\frac{u^3}{v^3}f''(0)+\frac{u^4}{v^4}f'''(0)+\frac{u^4}{v^4}S[k\,Re(4f''f'''+2f'f'''')-2Reff'''], \quad (28)$$

$$G(v,u)=\frac{u}{v}g(0)+\frac{u^2}{v^2}g'(0)+\frac{u^2}{v^2}S[Pr\,Re(n\,f'g+\,fg')]\ . \quad (29)$$

Applying the inverse Shehu transformation on both sides of (28,29), we get

$$f=S^{-1}\left[\frac{u^3}{v^3}f''(0)+\frac{u^4}{v^4}f'''(0)+\frac{u^4}{v^4}S[k\,Re(4f''f'''+2f'f'''')-2Reff''']\right] \quad (30)$$

$$g=1+S^{-1}\left[\frac{u^2}{v^2}g'(0)+\frac{u^2}{v^2}S[Pr\,Re(n\,f'g+\,fg')]\right] \quad (31)$$

By AGM, we must substitute (18) into (30,31), so, we get

$$\sum_{k=0}^{n}a_k\,t^k=S^{-1}\left[\frac{u^3}{v^3}A_1+\frac{u^4}{v^4}A_2+\frac{u^4}{v^4}S\left[k\,Re\left(\begin{array}{c}4\left(\sum_{k=0}^{n}a_k\,t^k\right)''\left(\sum_{k=0}^{n}a_k\,t^k\right)'''\\+2\left(\sum_{k=0}^{n}a_k\,t^k\right)'\left(\sum_{k=0}^{n}a_k\,t^k\right)''''\\-2Re\left(\sum_{k=0}^{n}a_k\,t^k\right)\left(\sum_{k=0}^{n}a_k\,t^k\right)'''\end{array}\right)\right]\right], \quad (32)$$

$$\sum_{k=0}^{n}b_k\,t^k=1+S^{-1}\left[\frac{u^2}{v^2}B+\frac{u^2}{v^2}S\left[Pr\,Re\left(\begin{array}{c}n\left(\sum_{k=0}^{n}a_k\,t^k\right)'\left(\sum_{k=0}^{n}b_k\,t^k\right)\\+\left(\sum_{k=0}^{n}a_k\,t^k\right)\left(\sum_{k=0}^{n}b_k\,t^k\right)'\end{array}\right)\right]\right], \quad (33)$$

where $A_1=f''(0)$, $A_2=f'''(0)$ and $B=g'(0)$.

When $n=4$, after simplification, Equations (32) and (33) becomes:

$$\Psi\big(f(t)\big)=48\mathrm{Ret}^5\mathrm{a}_4^2-1344\mathrm{Rekt}^3\mathrm{a}_4^2+60\mathrm{Ret}^4a_3a_4-1008\mathrm{Rekt}^2a_3a_4+48\mathrm{Ret}^3a_2a_4+12\mathrm{Ret}^3\mathrm{a}_3^2-288\mathrm{Rekta}_2a_4-144\mathrm{Rekta}_3^2+\cdots=0 \quad (34)$$

$$\Phi\big(g(t)\big)=2Repra_0b_1+8Reprt^7a_4b_4+8Reprt^6a_3b_4++6\ \mathrm{Re\ pr\ t}^6a_4b_3+8\ \mathrm{Re\ pr\ t}^5a_2b_4+6\ \mathrm{Re\ pr\ t}^5a_3b_3+4\ \mathrm{Re\ pr\ t}^5a_4b_2+\cdots=0 \quad (35)$$

The constant coefficients of (34,35) which are $\{a_0,\dots,a_4,b_0,\dots,b_4\}$ can be computed by applying boundary conditions in the form of:

$f(0)=0\Rightarrow a_0=0$

$\Psi\big(f(0)\big)\Rightarrow a_1=0$

$\Psi'\big(f(0)\big)\Rightarrow a_2=\frac{8kRe-1+\sqrt{64Re^2k^2+32Rek+1}}{8kRe}$

$\Psi''\big(f(0)\big)\Rightarrow a_3=-\frac{8kRe-1+\sqrt{64Re^2k^2+32Rek+1}}{4kRe}+4$

$\Psi'''\big(f(0)\big)\Rightarrow a_4=\frac{8kRe-1+\sqrt{64Re^2k^2+32Rek+1}}{8kRe}-3$

$g(0)=1\Rightarrow b_0=1$

$\Phi\big(f(0)\big)\Rightarrow b_1=\frac{8NkRe-N+N\sqrt{64Re^2k^2+32Rek+1}pr-48prReN-48k}{8NkRe-N+N\sqrt{64Re^2k^2+32Rek+1}pr-8kRe-1+\sqrt{64Re^2k^2+32Rek+1}pr+48k}$

$\Phi'\big(g(0)\big)\Rightarrow b_2=0$

$\Phi''\big(f(0)\big)\Rightarrow b_3=\frac{8NkRe-N+N\sqrt{64Re^2k^2+32Rek+1}pr}{24k}$

$\Phi'''\big(f(0)\big)\Rightarrow a_4=\frac{-1}{12}\left(prRe\left(N^2pr\big(8kRe-1+\sqrt{64Re^2k^2+32Rek+1}+\cdots\big)\right)\right)$

Then,

$$f(t)=\frac{8kRe-1+\sqrt{64Re^2k^2+32kRe+1}}{8kRe}t^2-\left(\frac{8kRe-1+\sqrt{64Re^2k^2+32kRe+1}}{4kRe}\right)t^3+4t^3+\frac{8kRe-1+\sqrt{64Re^2k^2+32kRe+1}}{8kRe}t^4-3t^4 \quad (36)$$

$$g(t)=1+\frac{8NkRe-N+N\sqrt{64Re^2k^2+32Rek+1}\mathrm{pr}-48prReN-48k}{8NkRe-N+N\sqrt{64Re^2k^2+32Rek+1}pr-8kRe-1+\cdots}t+\frac{8NkRe-N+N\sqrt{64Re^2k^2+32Rek+1}pr}{24k}t^3+\cdots \quad (37)$$

Now, take the Padé approximant of equation (36) and (37) with [3,4] and [0,4] respectively, we get the approximate solutions of the system (7,11):

$$f(t)_{[3,4]}=\frac{\left(0.125000000\left(1.441792\times10^6Re^5k^5-2.1299210^5\sqrt{64Re^2k^2+32kRe+1}Re^4k^4+\cdots\right)\right)}{1+\left(1.31072\times10^5Re^5k^5-36864\sqrt{64Re^2k^2+32kRe+1}Re^4k^4+3840\,(64Re^2k^2+32\,k\,Re+1)Re^3k^3+\cdots\right)}$$

$$g(t)_{[0,4]} = \frac{\left(1.0000\times10^{44}\left(576\,N^2\sqrt{64Re^2k^2+32kRe+1}Re\,k^2pr^4+13824.N\,(64.RRe^2k^2+32.k\,RRe+1)Re\,k^3pr^3+\cdots\right)\right)}{5.76000000\times10^{46}N^2\sqrt{64Re^2k^2+32kRe+1}Rek^2pr^4+1.38240000\times10^{48}N(64Re^2k^2+32kRe+1)Rek^3pr^3+\cdots}$$

4.2. q-HALPM

Now, we will take the model in the Equations (7,11) to apply the method to it as follows:

By applying the q-homotopy property on Equations (7,11), we obtained

$$(1-np)\left[L_1\left(f(t)\right)-L_1\left(f_0(t)\right)\right]+hp[f''''+2Reff'''-k\,Re(4f''f'''+2f'f'''')]=0 \quad (38)$$

$$(1-np)\left[L_2\left(g(t)\right)-L_2\left(g_0(t)\right)\right]+hp[g''-Pr\,Re(n\,f'\,g+\,fg')]=0 \quad (39)$$

Taking $L_1^{-1}=\int_0^t\int_0^t\int_0^t\int_0^t(.)\,dtdtdtdt$ and $L_2^{-1}=\int_0^t\int_0^t(.)\,dtdt$ for both sides of Equations (38) and (39) we have:

$$f=f(0)+tf'(0)+\frac{t^2}{2}f''(0)+\frac{t^3}{6}f'''(0)-pL_1^{-1}[2Reff'''-k\,Re(4f''f'''+2f'f'''')] \quad (40)$$

$$g=g(0)+tg'(0)+pL_2^{-1}[Pr\,Re(n\,f'g+\,fg')] \quad (41)$$

Now, assuming that $f(t)=\sum_{k=0}^{\infty}p^i\tau_k(t)$, $g(t)=\sum_{k=0}^{\infty}p^i\mu_k(t)$, then we get:

$$\sum_{k=0}^{\infty}p^i\tau_k(t)=\frac{t^2}{2}A_1+\frac{t^3}{6}A_2-pL_1^{-1}\begin{bmatrix}2Re\left(\sum_{k=0}^{\infty}p^i\tau_k(t)\right)\left(\sum_{k=0}^{\infty}p^i\tau_k(t)\right)'''\\-k\,Re\begin{pmatrix}4\left(\sum_{k=0}^{\infty}p^i\tau_k(t)\right)''\left(\sum_{k=0}^{\infty}p^i\tau_k(t)\right)'''\\+2\left(\sum_{k=0}^{\infty}p^i\tau_k(t)\right)'\left(\sum_{k=0}^{\infty}p^i\tau_k(t)\right)''''\end{pmatrix}\end{bmatrix}, \quad (42)$$

$$\sum_{k=0}^{\infty}p^i\mu_k(t)=1+tB+pL_2^{-1}\left[Pr\,Re\begin{pmatrix}n\left(\sum_{k=0}^{\infty}p^i\tau_k(t)\right)'\left(\sum_{k=0}^{\infty}p^i\mu_k(t)\right)\\+\left(\sum_{k=0}^{\infty}p^i\tau_k(t)\right)\left(\sum_{k=0}^{\infty}p^i\mu_k(t)\right)'\end{pmatrix}\right], \quad (43)$$

where $A_1=f''(0), A_2=f'''(0)$ and $B=g'(0)$.

We Equation the terms in Equations (42) and (43) that have the same powers p , we get

$\tau_0=24Re\left(-\frac{1}{420}t^7+\frac{1}{5}kt^5+\frac{1}{120}t^6-\frac{1}{2}kt^4\right)+\frac{1}{6}\left(\frac{288}{5}kRe-\frac{108}{35}Re\right)t^3+\frac{1}{2}\left(-\frac{24}{5}kRe+\frac{26}{35}Re\right)t^2$

$\mu_0=2Repr((\frac{1}{20}(3N-2))t^2+(\frac{1}{12}(-6N+3))t^4+\frac{1}{2}Nt^3)+(-\frac{3}{10}NRepr-\frac{3}{10}prRe)t$

$\tau_1=-\frac{48}{35}Re^2(\frac{1}{220}t^{11}-\frac{1}{40}t^{10}+(\frac{1}{3024}(-1848k+105))t^9+\frac{11}{4}t^8k+\cdots$

$\mu_1=-\left(\frac{1}{35}\right)prRe^2\left(\frac{1}{72}(63N^2pr-252N*pr-14N+140pr+4)\right)t^9+\cdots$

$\tau_2=\left(\frac{4}{13475}\right)Re^3\left(-\left(\frac{1051}{390}\right)t^{15}+\left(\frac{1051}{52}\right)t^{14}+\left(\frac{1}{17160}(9880640k-858550)\right)t^{13}\right)+\cdots$

$\mu_2=\left(\frac{1}{485100}\right)Re^3pr\left(\frac{1}{156}(72765N^3pr^2-727650N^2pr^2-74382N^2pr+1908060Npr^2+223608Npr-970200pr^2+33264N-83160pr-6048)\right)t^{13}+\cdots$

⋮

Then the solution of Equations (7,11) is given by substituting the τ_k and μ_k in $f(t)=\sum_{k=0}^{\infty}p^k\tau_k(t)$ and $g(t)=\sum_{k=0}^{\infty}p^k\mu_k(t)$

$f(t)=-2t^3+3t^2+24Re\left(-\left(\frac{1}{420}\right)t^7+\left(\frac{1}{5}\right)kt^5+\left(\frac{1}{120}\right)t^6-\left(\frac{1}{2}\right)kt^4\right)+\left(\frac{1}{6}\left(\left(\frac{288}{5}\right)kRe-\left(\frac{108}{35}\right)Re\right)\right)t^3+\left(\frac{1}{2}\left(-\left(\frac{24}{5}\right)kRe+\left(\frac{26}{35}\right)Re\right)\right)t^2-\left(\frac{48}{35}\right)Re^2\left(\left(\frac{1}{220}\right)t^{11}-\left(\frac{1}{40}\right)t^{10}+\left(\frac{1}{3024}(-1848k+105)\right)t^9+\left(\frac{11}{4}\right)t^8k+\left(\frac{1}{840}(18480k^2-2646k+18)\right)t^7+\left(\frac{1}{360}(-27720k^2+294k-20)\right)t^6+\left(\frac{1}{120}(11592k^2-216k)\right)t^5\right)+\left(\frac{1}{24}\left(\left(\frac{8064}{5}\right)k^2Re^2-\left(\frac{768}{7}\right)Re^2k\right)\right)t^4+\left(\frac{1}{6}\left(-\left(\frac{8928}{175}\right)k^2Re^2+\left(\frac{1448}{175}\right)Re^2k-\left(\frac{138}{539}\right)Re^2\right)\right)t^3+\left(\frac{1}{2}\left(-\left(\frac{576}{175}\right)k^2Re^2+\left(\frac{32}{35}\right)Re^2k+\left(\frac{416}{13475}\right)Re^2\right)\right)t^2+\cdots$

$g(t)=-t+1+2\,Re\,pr\,\left(\frac{1}{20}(3\,n-2)t^5+\frac{1}{12}(-6\,n+3)t^4+\frac{1}{2}n\,t^3\right)+\left(-\frac{3}{10}n\,Re\,pr-\frac{3}{10}pr\,Re\right)t-\frac{1}{35}Re^2pr\,\left(\frac{1}{72}(63\,n^2pr-252\,n\,pr-14\,n+140\,pr+4)t^9+\frac{1}{56}(-273\,n^2pr+1022\,n\,pr+56\,n-490\,pr-14)t^8+\frac{1}{42}(420\,n^2pr+840\,n\,k-1365\,n\,pr-42\,n-336\,k+420\,pr)t^7+\frac{1}{30}(-210\,n^2pr-2520\,n\,k+630\,n\,pr+840\,k)t^6+\frac{1}{20}(-63\,n^2pr+2688\,n\,k-21\,n\,pr-54\,n-672\,k+42\,pr+36)t^5+\frac{1}{12}(63\,n^2pr-1176\,n\,k+80\,n+168\,k-63\,pr-26)t^4+\frac{1}{6}(168\,n\,k-26\,n)t^3\right)+\left(\frac{11}{350}Re^2pr^2n^2+\frac{2}{175}Re^2pr\,n\,k+\frac{11}{175}Re^2pr^2n-\frac{101}{6300}Re^2pr\,n+\frac{2}{175}Re^2pr\,k+\frac{2}{1575}Re^2pr^2-\frac{101}{6300}Re^2pr\right)t+\cdots$

Now, by taken Laplace transform of f and g afterward us reception Padé approximate we have

$F(s)_{[3,3]}=\frac{A_1}{A_2}$ and, $G(s)_{[3,3]}=\frac{A_3}{A_4}$, where

$A_1 = (230473242313767578125(-1296 - \left(\frac{22464}{35}\right)Re - \left(\frac{95080416}{6131125}\right)Re^3 + \left(\frac{497664}{875}\right)k^3Re^3 + \left(\frac{8771328}{67375}\right)k^2Re^3 \ldots$

$A_2 = (s^3(-184905389833445531250000Re + \frac{1}{s}(-50256336723962118750\ Re - 107111464121762100\ Re^3 + \cdots$

$A_3 = (1607678790968250(\frac{1}{s}(12 + \left(\frac{52}{35}\right)Re - 24N - \left(\frac{2312396}{13138125}\right)N^4Re^5kpr^3 - \left(\frac{259380500326}{724963379765625}\right)N^3Re^7kpr^2 + \cdots$

$A_4 = -28296199081069920000N^4Re^5kpr^3 - 57520219752293760N^3Re^7kpr^2 - 385842909832380000N + \cdots$

Later, taking invers Laplace transformation for $F(s)_{[3,3]}$ and $G(s)_{[3,3]}$ to get :

$f(t) = \frac{9}{6131125}\left(\frac{e^{\alpha t}}{3054291432192000Re^6k^6\alpha^2 - 8144777152512000Re^6k^6\alpha - 20487552269184000Re^6k^5\alpha^2 + \cdots}\right)$

Where

$\alpha = \sqrt{150878647120324707904 32Re^3k^3 - 5125367677177197450 0Re^3 + \cdots}$

$g(t) = \frac{1}{63063000}(e^{\alpha t}(-243324114227593799400 + (-250815176775998050986N^{12}Re^{11}pr^{11} -$
$1340994494806326958752N^{11}Re^{11}kpr^{10} + \cdots)$

Where

$\alpha = \sqrt{-6469616557853729280N^4Re^5kpr^3 - 747291790964759040N^3Re^7kpr^2 + \cdots}$

4.3. PYRDTM

We have the final method to apply it to the mathematical model in the Equations (7,11) as follows

Applying the Yang transform to both sides of Equation (7,11) under the initial condition given in Equations (8,12), we obtain

$$F(s) = sf(0) + s^2f'(0) + s^3f''(0) + s^4f'''(0) + s^4Y[k\ Re(4f''f''' + 2f'f'''') - 2Reff'''], \quad (44)$$

$$G(s) = \mathrm{s}g(0) + s^2g'(0) + s^2Y[Pr\ Re(n\ f'g + \ fg')]\,. \quad (45)$$

By performing the inverse Yang transform on Equation s (44,45), we obtain:

$$f = \frac{1}{2}t^2A_1 + \frac{1}{6}t^3A_2 + Y^{-1}\left[s^4Y[k\ Re(4f''f''' + 2f'f'''') - 2Reff''']\right]\,, \quad (46)$$

$$g = 1 + t\mathrm{B} + Y^{-1}\left[s^2Y[Pr\ Re(n\ f'g + \ fg')]\right]\,, \quad (47)$$

where $A_1 = f''(0)\,, A_2 = f'''(0)$ *and* $B = g'(0)$.

By utilizing the reduced differential transform method on Equation s (46,47), we obtain:

$$F_{k+1} = \frac{1}{2}t^2A_1 + \frac{1}{6}t^3A_2 + Y^{-1}\left[s^4Y\left[k\ Re\left(\begin{array}{c} 4\sum_{r=0}^{k}F_{r+2}(r+1)(r+2)\,F_{k-r+3}(k-r+1)(k-r+2)(k-r+3) \\ +2\sum_{r=0}^{k}F_{r+1}(r+1)F_{k-r+4}(k-r+1)(k-r+2)(k-r+3)(k-r+4) \\ -2Re\sum_{r=0}^{k}F_r\,F_{k-r+3}(k-r+1)(k-r+2)(k-r+3) \end{array}\right)\right]\right] \quad (48)$$

$$G_{k+1} = 1 + t\mathrm{B} + Y^{-1}\left[\boldsymbol{s^2}Y\left[Pr\ Re\left(\begin{array}{c} n\sum_{r=0}^{k}F_{k-r+1}(k-r+1)\ G_r \\ +\sum_{r=0}^{k}G_{k-r+1}(k-r+1)\ F_r \end{array}\right)\right]\right] \quad (49)$$

With $F_0 = 0, F_1 = 0, F_2 = 1.361107895t^2, F_3 = .2657143550t^3$ and
$G_0 = 1, G_1 = -1.338712981t$.

Then from the Equation s (48,49), we get

$F_0 = 0$
$F_1 = 0$
$F_2 = 1.361107895t^2$
$F_3 = 0.2657143550t^3$
$F_4 = 2.893327251kRet^6$
$F_5 = 126.0201781Re^2k^2t^9 + 1.452427580Rekt^7$
$\vdots$
$G_0 = 1$
$G_1 = -1.338712981t$
$G_2 = 0$
$G_3 = 0.9074052633prReNt^3$

$G_4 = -\big(0.7117806375(N - 1.279982000)\big)prRet^4$
$G_5 = 1.653329857prRe^2t^7Nk - \big(0.2134291539(N - .6666666662)\big)prt^5Re$
⋮
The solutions series obtained by YRDTM is

$$f = \sum_{k=0}^{\infty} F_k = 1.361107895t^2 + 0.2657143550t^3 + 2.893327251kRet^6 + 126.0201781Re^2k^2t^9 + 1.452427580Rekt^7 + 13722.16474Re^3t^{12}k^3 + 267.2783193Re^2t^{10}k^2 + \cdots \quad (50)$$

$$g = \sum_{k=0}^{\infty} G_k = 1 - 1.338712981t + 0.9074052633prReNt^3 - \big(0.7117806375(N - 1.279982000)\big)prRet^4 + 1.653329857prRe^2t^7Nk - \big(0.2134291539(N - 0.6666666662)\big)prt^5Re + \cdots \quad (51)$$

Now, take the Padé approximant of Equation (50), with $i = 3$, $j = 4$, and take the Padé approximant of equation. (51), with $i = 0$, $j = 4$ we get the solutions of the system (7,11) as
$f(t)_{[3,4]} = \frac{B_1}{B_2}$ and, $g(t)_{[0,4]} = \frac{1}{B_3}$, where
$B_1 = (8 \times 10^{34}(9.930423493Rek - 2.482605873Re)\frac{t^2}{5.836670865\times10^{35}Rek - 1.459167716\times10^{35}Re - 3.987953234\times10^{32}} + \cdots$
$B_2 = 1 + (-1.790532934 \times 10^{35}Rek - 4.069393031 \times 10^{33}Re)\frac{t}{5.836670865\times10^{35}Rek - 1.459167716\times10^{35}Re - 3.987953234\times10^{32}} + \cdots$
$B_3 = 1 + (-1.717729773prReN - 0.9110664039prRe + 3.211810388)t^4 + (2.399177743 - 0.9074052633prReN)t^3 + \cdots$

5. Results and discussion

Three new existing approximation methods were used to solve the problem of turbine disk cooling by non-Newtonian fluid flow in the porous wall of an axisymmetric channel (Figure 1). Approximate solutions were obtained, and Tables (3-8) show the results obtained using these methods. Tables (1) and (2) also show a comparison of errors between the three methods in addition to CHPM [13]. the results obtained from the three methods indicate that the q-homotopy approach demonstrates superior efficiency in terms of both accuracy and convergence rate. This method achieved negligible or nearly zero errors, underscoring its effectiveness. In contrast, although the other methods produced satisfactory outcomes, they did not achieve the same level of precision and computational efficiency exhibited by the q-homotopy method. Converging from Figures 3 and 4, we can see that the Reynolds number (Re) and the cross-viscosity parameter (k) have the same effect on the velocity, as their increase leads to an increase in the velocity in the
y-direction, and the maximum velocity in the *x*-direction tends to the warm plate (y=0). Figure 5 shows the effect of Reynolds number (Re), cross-linked viscosity parameter (k), Prandtl number (pr), and power law index (n) on the temperature distribution. This figure shows that the higher it is, the lower the temperature distribution.

Table 1. Comparison of the error between the methods mentioned below for f

$Method$	Re	k	L_2	L_∞
SAGPM	0.01	0.01	0.1063837916	0.103819950
	0.1	0.01	0.3552495559	0.346688068
	0.5	0.1	0.1227072354e-2	0.1197500e-2
	1	0.1	0.1063837916	0.103819950
q-HALPM	0.01	0.01	$7.631673732 \times 10^{-6}$	$0.1451228316e-5$
	0.1	0.01	0.9539592179e-4	0.1814035398e-3
	0.5	0.1	$2.168888355 \times 10^{-9}$	$3.746156400 \times 10^{-9}$
	1	0.1	0.2168888355e-3	0.3746156400e-3
PYRDTM	0.01	0.01	0.9349148830e-2	0.2893327251e-1
	0.1	0.01	0.4674574417e-1	0.1446663626
	0.5	0.1	0.9349148830e-4	0.2893327251e-3
	1	0.1	0.9349148830e-2	0.2893327251e-1
CHPM	0.01	0.01	0.5099801859e-2	0.170090314e-1
	0.1	0.01	0.5241776027e-1	0.1759097868
	0.5	0.1	0.6039242226e-3	0.1663236059e-2
	1	0.1	0.5099801859e-2	0.170090314e-1

Table 2. Comparison of the error between the methods mentioned below for g

$Method$	n	Re	k	pr	L_2	L_∞
Error of SAGPM	1	0.01	0.01	0.01	0.1416985076e-2	0.4480900250e-2
	2	0.1	0.01	0.1	0.1125645185	0.2906403369
	3	0.5	0.1	0.5	0.1117074541e-3	0.2497854610e-3

	4	1	0.1	1	1.803927948	3.607855897
Error of q-HALPM	1	0.01	0.01	0.01	$7.055130671 \times 10^{-8}$	$3.155150354 \times 10^{-6}$
	2	0.1	0.01	0.1	0.3291961245e-4	0.1313888698e-3
	3	0.5	0.1	0.5	$6.772011223 \times 10^{-13}$	$2.304450836 \times 10^{-13}$
	4	1	0.1	1	0.2482841529e-1	0.8070223202e-1
Error of PYRDTM	1	0.01	0.01	0.01	$2.785103254 \times 10^{-7}$	$1.245536040 \times 10^{-7}$
	2	0.1	0.01	0.1	0.2870523545e-5	0.1281237178e-4
	3	0.5	0.1	0.5	$1.412773954 \times 10^{-7}$	$6.197894764 \times 10^{-7}$
	4	1	0.1	1	0.7278036682e-3	0.3097689834e-2
Error of CHPM	1	0.01	0.01	0.01	0.2179985094e-2	0.5945262275e-2
	2	0.1	0.01	0.1	0.2132580049	0.5851376107
	3	0.5	0.1	0.5	0.1171542426e-3	0.3211343167e-3
	4	1	0.1	1	3.649711398	10.12419691

Now we will review the problem diagrams for each method as follows:

6.1. SAGPM:

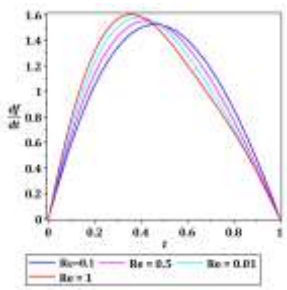

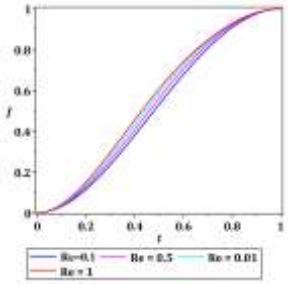

(b) **(a)**

Fig.2: The impact of the Reynolds number on the y-direction(a) and x-direction(b) velocity components for $k = 0.01$ and $k = 0.1$.

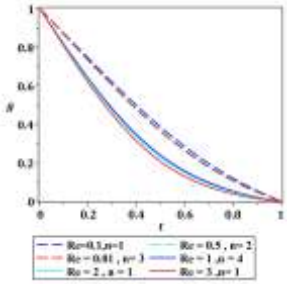

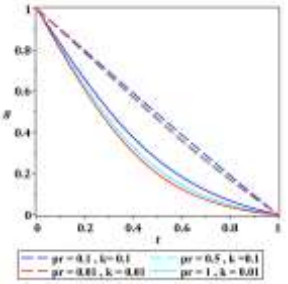

(b) **(a)**

Fig.3: The impact of the Re, n, pr and k on the temperature distribution components.

6.2. q-HALPM

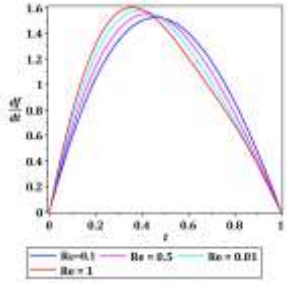

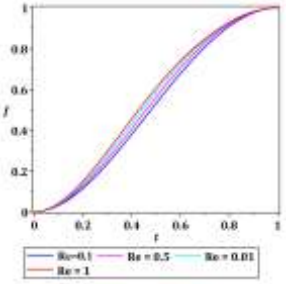

(b) **(a)**

Fig.4: The impact of the Reynolds number on the y-direction(a) and x-direction(b) velocity components for $k = 0.01$ and $k = 0.1$.

(b) **(a)**

Fig.5: The impact of the Re, n, pr and k on the temperature distribution components.

6.3. PYRDTM

(b) **(a)**

Fig.6: The impact of the Reynolds number on the y-direction(a) and x −direction(b) velocity components for $k = 0.01$ and $k = 0.1$.

(b) **(a)**

Fig.7: The impact of the Re, n, pr and k on the temperature distribution components .

5. Convergent analysis

In this section, we perform a convergence analysis of the approximate analytical solution derived using the three methods. To achieve this, we study a system of nonlinear ordinary differential Equations, represented by equations (7) and (11) as follows:

$$\left.\begin{aligned} f(t) &= F\big(f(t), g(t)\big) \\ g(t) &= G\big(f(t), g(t)\big) \end{aligned}\right\} \tag{52}$$

Where F and G are non-linear operators. The solutions of the model using the three methods above are equation

univalent to the following equation

$$\mathcal{S}_{n_1} = \sum_{k=0}^{n_1} \mathcal{u}_k \tag{53}$$

$$\mathcal{M}_{n_2} = \sum_{k=0}^{n_2} \mathcal{v}_k \tag{54}$$

Theorem 5.1 (Convergence of the Turbine Disk Cooling Problem)
Let F and G be operators mapping a Hilbert space H into H itself, and let f and g represent the exact solutions of equations (7) and (11), respectively. The approximate solutions, $\sum_{k=0}^{n_1} \mathcal{u}_k$, and $\sum_{k=0}^{n_2} \mathcal{v}_k$ converge to the exact solutions , f and g, respectively ,when under the conditions , $\exists\ 0 \le \vartheta < 1$, $\|\mathcal{u}_{k+1}\| \le \vartheta\|\mathcal{u}_k\|$, $\forall k \in \mathbb{N} \cup \{0\}$ and $\exists\ 0 \le \delta < 1$, $\|\mathcal{v}_{k+1}\| \le \delta\|\mathcal{v}_k\|$, $\forall k \in \mathbb{N} \cup \{0\}$.

Proof: First, we demonstrate that for f,

$$\left\|\mathcal{S}_{n_1+1} - \mathcal{S}_{n_1}\right\| = \left\|\mathcal{u}_{n_1+1}\right\| \le \vartheta\left\|\mathcal{u}_{n_1}\right\| \le \vartheta^2\left\|\mathcal{u}_{n_1-1}\right\| \le \cdots \le \vartheta^{n_1}\|\mathcal{u}_1\| \le \vartheta^{n_1+1}\|\mathcal{u}_0\|. \tag{55}$$

Now for n_1 , $m_1 \in \mathbb{N}$, $n_1 \ge m_1$,we have

$$\begin{aligned}\left\|\mathcal{S}_{n_1} - \mathcal{S}_{m_1}\right\| &= \left\|\left(\mathcal{S}_{n_1} - \mathcal{S}_{n_1-1}\right) + \left(\mathcal{S}_{n_1-1} - \mathcal{S}_{n_1-2}\right) + \cdots + \left(\mathcal{S}_{m_1+1} - \mathcal{S}_{m_1}\right)\right\| \\ &\le \left\|\mathcal{S}_{n_1} - \mathcal{S}_{n_1-1}\right\| + \left\|\mathcal{S}_{n_1-1} - \mathcal{S}_{n_1-2}\right\| + \cdots + \left\|\mathcal{S}_{m_1+1} - \mathcal{S}_{m_1}\right\| \\ &\le \vartheta^{n_1}\|\mathcal{u}_0\| + \vartheta^{n_1-1}\|\mathcal{u}_0\| + \cdots + \vartheta^{m_1+1}\|\mathcal{u}_0\| \\ &\le (\vartheta^{m_1+1} + \vartheta^{m_1+2} + \cdots + \vartheta^{n_1})\|\mathcal{u}_0\| = \\ \vartheta^{m_1+1}\frac{1-\vartheta^{n_1+m_1}}{1-\vartheta}\|\mathcal{u}_0\|\end{aligned} \tag{56}$$

Hence , $\lim_{n_1,m_1\to\infty}\left\|\mathcal{S}_{n_1} - \mathcal{S}_{m_1}\right\| = 0$, this mean $\{\mathcal{S}_{n_1}\}_{n_1}^{\infty}$ is a Cauchy sequence in the Hilbert space ,then there exists $\mathcal{S} \in H$, such that $\lim_{n_1,\to\infty} \mathcal{S}_{n_1} = \mathcal{S}$, where $\mathcal{S} = f$.

The proof for g follows a similar procedure. ■

According to **Theorem 5.1**, the convergence of the approximate solutions depends on calculating the parameter values ϑ^{n_1} to satisfy the following relationship:

$$\vartheta^{n_1} = \begin{cases} \dfrac{\left\|\mathcal{u}_{n_1+1}\right\|}{\left\|\mathcal{u}_{n_1}\right\|}, & \|\mathcal{u}_0\| \ne 0, \quad n_1 = 2,3,4,\ldots \\ 0, & \text{otherwise} \end{cases} \tag{57}$$

where $\vartheta = \frac{\|\mathcal{u}_{n_1+1}\|}{\|\mathcal{u}_{n_1}\|} < 1$.

By applying the above relationship, the convergence of the solutions produced by the three methods can now be determined as follows:

5.1. SAGPM:

Table 3. convergence of analytical approximate solutions for f

Re	k	ϑ^1	ϑ^2
0.01	0.01	0.6661342321	0.5994678626e-3
0.1	0.01	0.6613963051	0.5976403537e-2
0.5	0.1	0.4924501523	0.2653311922
1	0.1	0.4000000000	0.2000000000

Table 4. convergence of analytical approximate solutions for g

Re	k	pr	n	δ^1	δ^2
0.01	0.01	0.01	1	0.9995508360e-4	0.4993762712e-4
0.1	0.01	0.1	2	0.1982147479e-1	0.1481270174e-1
0.5	0.1	0.5	3	0.5710889259	0.4320339489
1	0.1	1	4	2.250000000	1.925000000

5.2. q-HALPM:

Table 5. convergence of analytical approximate solutions for f

Re	k	ϑ^1	ϑ^2
0.01	0.01	0.2840512145e-3	0.2722483140e-5
0.1	0.01	0.2840512145e-2	0.2722483140e-3
0.5	0.1	0.1288934946	0.8783299435e-2
1	0.1	0.2577869893	0.3513319775e-1

Table 6. convergence of analytical approximate solutions for g

Re	k	pr	n	δ^1	δ^2
0.01	0.01	0.01	1	0.4212753274e-3	0.1127772672e-5
0.1	0.01	0.1	2	0.1096140060e-2	0.3654942119e-3
0.5	0.1	0.5	3	0.9592202424e-1	0.1333512589e-1
1	0.1	1	4	0.5568706417	0.3632358743

5.3. PYRDTM:

Table 7. convergence of analytical approximate solutions for f

Re	k	ϑ^1	ϑ^2
0.01	0.01	0.2496906195e-2	0.2045291406e-3
0.1	0.01	0.2496504310e-1	0.2951371679e-2
0.5	0.1	0.1247309475	0.3493991610e-1
1	0.1	0.2492034521	0.1203148005

Table 8. convergence of analytical approximate solutions for g

Re	k	pr	n	δ^1	δ^2
0.01	0.01	0.01	1	0.1109341948e-4	1.074331209e-8
0.1	0.01	0.1	2	0.2218683896e-2	0.2762812641e-4
0.5	0.1	0.5	3	0.8320064605e-1	0.8249945618e-2
1	0.1	1	4	0.4437367791	0.1043710034

6. Conclusions :

In this work, three major techniques—SAGPM, q-HALPM, and PYRDTM—are applied to find the solutions of the turbine disk cooling problem. The investigations consider the influences of the significant parameters, such as injection Reynolds number (Re), the cross-viscosity parameter (k), the Prandtl number (Pr), and the power-law exponent (n), on the speed and temperature distributions. The results reveal that an increase in the Reynolds number increases the velocity with more pronounced curvature and a drop in temperature distribution. For small Reynolds numbers, the velocity reaches its maximum at the center of the channel. Besides, larger Prandtl numbers and power-law exponents lead to a conspicuous decline in temperature distribution.

The q-HALPM had better convergence and accuracy compared to SAGPM and PYRDTM, as seen in Tables 1 and 2. The comparison showed that all three methods were reliable, but q-HALPM always had the lowest error rates. These results demonstrate that such methods can be powerful tools in the solution of complicated fluid flow problems and in developing applications in engineering and applied sciences. It is also found that an increase in the cross-linking viscosity parameter causes acceleration, while a decrease in temperature spread causes deceleration.

Funding: This research received no external funding.

Conflicts of Interest: The authors declare no conflict of interest.

Publisher's Note: All claims expressed in this article are solely those of the authors and do not necessarily represent those of their affiliated organizations, or those of the publisher, the editors and the reviewers.

References

Bird, R. B., Armstrong, R. C., and Hassager, O., Dynamics of Polymeric Liquids, Fluid Mechanics, John Wiley & Sons, 1st Edition, (1987).

[1] Schlichting, H., and Gersten, K., Boundary-Layer Theory, Springer, 9th Edition, pp. 821, (2016).

[2] White, F. M., Viscous Fluid Flow, McGraw-Hill, 3rd Edition, (2011).

[3] Bejan, A., Convection Heat Transfer, John Wiley and Sons, 4th Edition, (2013).

[4] Ayan, S., & Alveroğlu, B. (2024). Investigation of Power-Law Fluid on a Decelerated Rotating Disk. In Fundamental Journal of Mathematics and Applications (Vol. 7, Issue 3, pp. 147–157). Fundamental Journal of Mathematics and Applications. https://doi.org/10.33401/fujma.1524621

[5] Dogonchi, A. S., & Ganji, D. D. (2015). Investigation of heat transfer for cooling turbine disks with a non-Newtonian fluid flow using DRA. In Case Studies in Thermal Engineering (Vol. 6, pp. 40–51). Elsevier BV. https://doi.org/10.1016/j.csite.2015.06.002

[6] Arif, M. S., Shatanawi, W., & Nawaz, Y. (2023). Modified Finite Element Study for Heat and Mass Transfer of Electrical MHD Non-Newtonian Boundary Layer Nanofluid Flow. In Mathematics (Vol. 11, Issue 4, p. 1064). MDPI AG. https://doi.org/10.3390/math11041064

[7] Mirgolbabaee, H., Ledari, S. T., Sheikholeslami, M., & Ganji, D. D. (2017). Semi-analytical Investigation of Momentum and Heat Transfer of a Non-Newtonian Fluid Flow for Specific Turbine Cooling Application Using AGM. In International Journal of Applied and Computational Mathematics (Vol. 3, Issue S1, pp. 1463–1475). Springer Science and Business Media LLC. https://doi.org/10.1007/s40819-017-0416-3

[8] Navneet Kumar Singh, & Yadav, R. (2017). Investigation Of Heat Transfer Of Non-Newtonian Fluid In The Presence Of A Porous Wall. Zenodo. https://doi.org/10.5281/ZENODO.1140081

[9] Sheikhzadeh, G., Mollamahdi, M., & Abbaszadeh, M. (2018). Analytical study of flow field and heat transfer of a non-Newtonian fluid in an axisymmetric channel with a permeable wall. Journal of Computational & Applied Research in Mechanical Engineering (JCARME), 7(2). https://doi.org/10.22061/jcarme.2017.2003.1174

[10] Akinshilo, A. T., Sanusi, M., Sobamowo, M. G., & Olorunnisola, A. E. (2021). Thermal performance analysis of non-Newtonian fluid transport through turbine discs. In Heat Transfer (Vol. 51, Issue 1, pp. 451–469). Wiley. https://doi.org/10.1002/htj.22315

[11] Al-Griffi, T. A. J., & Al-Saif, A. J. (2022). Yang transform–homotopy perturbation method for solving a non-Newtonian viscoelastic fluid flow on the turbine disk. In ZAMM - Journal of Applied Mathematics and Mechanics / Zeitschrift für Angewandte Mathematik und Mechanik (Vol. 102, Issue 8). Wiley. https://doi.org/10.1002/zamm.202100116

[12] Abdul-Wahab, M. S., & Ali Al-Saif, A.-S. J. (2024). Chebyshev-Homotopy Perturbation Method for Studying the Flow and Heat Transfer of a Non-Newtonian Fluid Flow on the Turbine Disk. In Basrah Researches Sciences (Vol. 50, Issue 1, p. 17). College of Education for Pure Science, University of Basrah. https://doi.org/10.56714/bjrs.50.1.13

[13] Abdul-Wahab, M. S., & Al-Saif, A. S. J. (2018). A New Technique for Simulation the Zakharov–Kuznetsov Equation. In JOURNAL OF ADVANCES IN MATHEMATICS (Vol. 14, Issue 2, pp. 7912–7920). CIRWOLRD. https://doi.org/10.24297/jam.v14i2.7559

[14] A. S. J. Al-Saif and Mohammed S. Abdul-Wahab, (2019), Application of New Simulation Scheme for the Nonlinear Biological Population Model, Numerical and Computational Methods in Sciences, (Vol. 1 Jul., pp. 89-99). http://dx.doi.org/10.18576/ncmsel/010204

[15] Umesh, & Kumar, M. (2020). Approximate solution of singular IVPs of Lane–Emden type and error estimation via advanced Adomian decomposition method. In Journal of Applied Mathematics and Computing (Vol. 66, Issues 1–2, pp. 527–542). Springer Science and Business Media LLC. https://doi.org/10.1007/s12190-020-01444-2

[16] Al-Saif, A. S. J., & Al-Griffi, T. A. J. (2021). Analytical Simulation for Transient Natural Convection in a Horizontal Cylindrical Concentric Annulus. Journal of Applied and Computational Mechanics, 7(2). https://doi.org/10.22055/jacm.2020.35278.2617

[17] Al-Griffi, T., & Al-Saif, A. S. J. (2022). Akbari-Ganji Homotopy Perturbation Method for Analyzing the Pulsatile Blood Flow in Tapered Stenosis Arteries under the Effect of Magnetic Field together with the Impact of Mass and Heat Transfer. Journal of Computational Applied Mechanics, Online First. https://doi.org/10.22059/jcamech.2022.348399.757

[18] Yasir Ahmed Abdulameer, & Abdul-Sattar Jaber Ali Al-Saif. (2022). A Well-Founded Analytical Technique to Solve 2D Viscous Flow Between Slowly Expanding or Contracting Walls with Weak Permeability. In Journal of Advanced Research in Fluid Mechanics and Thermal Sciences (Vol. 97, Issue 2, pp. 39–56). Akademia Baru Publishing. https://doi.org/10.37934/arfmts.97.2.3956

[19] Al-Jaberi, A. K., Abdul-Wahab, M. S., & Buti, R. H. (2022). A new approximate method for solving linear and non- linear differential equation systems. In AIP Conference Proceedings. PROCEEDING OF THE 1ST INTERNATIONAL CONFERENCE ON ADVANCED RESEARCH IN PURE AND APPLIED SCIENCE (ICARPAS2021): Third Annual Conference of Al-Muthanna University/College of Science. AIP Publishing. https://doi.org/10.1063/5.0094138

[20] Al-Jaberi, A. K., Abdul-Wahab, M. S., & Buti, R. H. (2022). A new approximate method for solving linear and non- linear differential equation systems. In AIP Conference Proceedings. PROCEEDING OF THE 1ST INTERNATIONAL CONFERENCE ON ADVANCED RESEARCH IN PURE AND APPLIED SCIENCE (ICARPAS2021): Third Annual Conference of Al-Muthanna University/College of Science. AIP Publishing. https://doi.org/10.1063/5.0094138